SIMULATION-REAL-TIME-MODELS FOR THREE-DIMENSIONAL INTERACTION BETWEEN WIND AND AIRCRAFT

Dipl.-Ing. Wolfgang Kindel
Aerospace Institute
Flight Mechanic and Control
Berlin University of Technology
Marchstraße 12
D-10587 Berlin, Germany

Dipl.-Ing. Thomas Heintsch
Deutsche Aerospace Airbus GmbH
Flight Guidance and Control
P.O. Box 950109
D-21111 Hamburg, Germany

Abstract

The influence of atmospheric perturbations on aircraft motion is an important factor in flight simulation for training and research purposes. Conventional flight simulation models consider the wind vector only at the center of gravity. If the characteristic wave length of the wind phenomenon is significantly greater than the aircraft's dimensions, this simple model shows good results. For small sized wind phenomena like microbursts, wake vortices or stochastic disturbances like gust and turbulence a new approach considering the aircraft as a multi-point model and the wind phenomenon as spatial has to be applied.

Different approaches for the spatial modeling of wind-aircraft interaction are possible. The first one is a four-point aerodynamic model which considers the local wind vector at four significant points of the aircraft. The validity of this model is restricted to wind perturbations with a typical wave length not less than the sixfold size of the aircraft wing span. For smaller sized wind phenomena, e.g. for the investigation of the influence of wake vortices on a following aircraft, a more complex aerodynamic model is necessary, which is based on the linear lifting surface theory.

To reduce the required computation power of the simulation computer, a matrix-wind model was developed which uses pre-computed wind fields, so that spatial wind models of nearly unlimited complexity can be calculated. As the wake vortex flow field is a function of time, this wind model cannot be pre-computed. Therefore a real-time capable mathematical algorithm was developed, which describes the vortex development analytically.

This paper presents a survey of different approaches of the real-time modeling for the interaction of atmospheric and aircraft motion which are suitable for different research and training purposes.

1. Introduction

The influence of atmospheric perturbations on aircraft motion is of great interest since the beginning of aviation and is an important factor in its different disciplines, e.g. flight mechanics, flight guidance or loads investigations. Today structural damages are almost no more a problem with respect to flight safety but there are still accidents caused by atmospheric perturbations like wind shear or wake vortices. Therefore enhanced knowledge about wind-aircraft interaction phenomena is required. To improve flight safety systematic investigations have to be carried out with the pilot in the loop. Due to safety aspects and to assure selectable and reproducable conditions a flight simulator is required. The aircraft simulation model has to be designed with special regard to the interaction between wind and aircraft.

The scale of the atmospheric perturbations is a significant parameter concerning the required complexity for the description of the wind-aircraft interaction. Long periodic changes of the wind can be considered as quasistationary leading to steady solutions of the aircraft motion concerning e.g. range or fuel consumption computations. For these investigations the aircraft aerodynamics can be treated as an one-point model.

Medium scaled wind disturbances are investigated with respect to stability and control aspects. This is the scale range of thunderstorm or microburst scenarios, which are extreme examples of the well known wind shear phenomenon. In this scale range the influence of the wind disturbances should be considered at several points of the aircraft, e.g. left and right wing tip, center of gravity and tail.

The influence of short scaled atmospheric perturbations like gust and turbulence determine the structural load of the aircraft and is of interest for passenger comfort and in extreme situations for flight safety aspects. The influence of wake vortices on the motion of a following aircraft is a

typical example for this. In this scale range flight simulation requires a complex aerodynamic model which considers the wind vector at several points along the wing and tail plane span.

2. Nomenclature

a_i	coefficients for local distribution of the wind angle of attack in wing chord direction
b	wing span
b_{vn}	MULTHOPP coefficients
c_{Di}	local coefficient for induced drag
c_L	local lift coefficient
c_l	local rolling moment coefficient
c_m	local pitching moment coefficient
c_n	local yawing moment coefficient
dL	local lift force
i_{vn}	coefficients for the lifting surface model
j_{vn}	coefficients for the lifting surface model
l	local aerodynamic chord
l_μ	mean aerodynamic chord
s	semi wing span
u_W	horizontal component of the wind vector
x_{25}	local distance of quarter chord line from pitching moment reference axis
y	lateral coordinate
w_W	vertical component of the wind vector
A	wing surface
C_L	lift coefficient
C_D	drag coefficient
C_l	rolling moment coefficient
C_m	pitching coefficient
C_n	yawing coefficient
$\underline{\underline{K}}$	Matrix for lifting surface model
$\underline{V}$	airspeed vector
$\underline{V}_K$	flight path speed vector
$\underline{V}_W$	wind speed vector
α	angle of attack
α_W	wind angle of attack
Γ_0	total circulation
γ	dimensionless local circulation
γ	flight path angle
η	dimensionless lateral coordinate
λ	wave length
μ	local pitching moment coefficient
ρ	air density
ξ	dimensionless longitudinal coordinate
Δ	deviation
ϑ	angle
Λ	wing aspect ratio

Indices

*	wing trailing edge
**	wing quarter chord line

3. Aerodynamic Models

3.1 General

For the investigation of aircraft behaviour in a turbulent atmosphere a suitable aerodynamic model is required to describe the interaction between the aircraft aerodynamic and the surrounding atmosphere. The aircraft flight path speed corresponds to the sum of the airspeed, which is the aircraft motion related to the atmosphere, and the wind speed, which is the motion of the atmosphere related to earth:

$$\underline{V}_K = \underline{V} + \underline{V}_W \tag{3.1}$$

Changes in the wind speed vector in the first moment lead to a change in the aircraft's flow condition expressed by the airspeed vector but the flight path velocity vector remains constant due to the aircraft's inert behaviour. The change of airspeed vector results in aerodynamic forces and moments which let the aircraft move until the undisturbed condition for the airspeed is recovered. The influence of the wind disturbances then is contained in the change of the flight path speed vector. For the description of this interaction between wind disturbance and aircraft motion three aerodynamic models are presented which show significant differences in their complexity of describing this physical phenomenon.

3.2 One-Point Model

The most simple algorithm is the one-point model which considers the wind disturbance only at the aircraft center of gravity. This model shows realistic results only for a nearly constant wind velocity distribution along the aircraft surface and is suited for example for low frequent wind shear disturbances, where the wave length of the wind field is large compared to the aircraft's dimensions. For investigations of the aircraft's response to higher frequent wind phenomena with geometric scales in the range of the wing span the one point model shows poor precision. Here more complex aerodynamic models are required which consider the wind velocity distribution along the aircraft both in the longitudinal and in the lateral direction.

As the wind field can be devided into a mean wind component with low frequent changes and spatial distributed deviations of higher frequency, the one-point model however can be used to calculate the influence of the mean wind while the spatial wind deviations should be considered by multi-point models.

$$\underline{V}_W = \underline{V}_{W,mean} + \Delta\underline{V}_{W,spatial} \tag{3.2}$$

3.3 Four-Point Model

The four-point model is a linear algorithm, which approximates the wind velocity distribution along the aircraft by a linear function[3,4]. Here the wind vector is considered at four points of the aircraft (see fig. 3.1), which

are

- left wing tip
- wing aerodynamic center
- right wing tip
- aerodynamic center of the tail unit

Compared to the one-point model here additionally wind induced rolling and pitching moments are calculated. The accuracy of the four-point model is directly related to the expansion of the wind disturbance compared to the distance between the four reference points. Fig. 3.1 shows a sine shaped wind velocity distribution along the wing span together with the corresponding linearized approximation. To determine the accuracy and the limits of the four-point model the results of a rolling moment calculation are compared to the complete solution of the lifting surface model (see chapter 3.4) as reference.

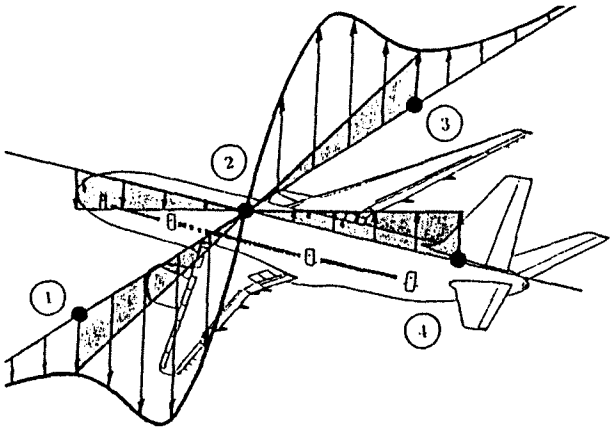

Fig. 3.1 Four-point model[5]

Fig. 3.2 shows the error versus the ratio of the wave length of the wind disturbance λ to the half wing span s, which is the distance between the reference points. The figure shows, that an error in the aerodynamic calculation of less than 10% requires a wave length which is about the sixfold size than the semi wing span[5]. For higher frequent wind disturbances the error of the four-point model rises progressively so that the results are no more realistic.

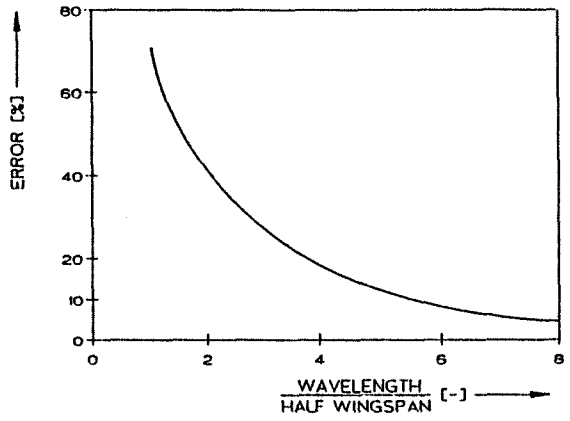

Fig. 3.2 Error of the four-point model[5]

3.4 Lifting Surface Aerodynamic Model

Theory

The lifting surface model is based on the assumption that the surface of the wing must be a stream layer of the airflow. On the stream layer the velocity components perpendicular to the surface are equal zero. If the wing can be replaced by a system of potential vortices in the lateral and longitudinal direction (horse shoe vortices) this so called kinematic flow condition leads to a determination of the circulation distribution.

According to KUTTA-JOUKOVSKY's law the lifting force distribution along the wing span can be calculated from

$$dL(y) = \rho \cdot V \cdot \gamma(y) \cdot dy \tag{3.3}$$

which is the basis of the lifting surface model. The kinematic flow condition on the surface leads to an integral equation for the circulation distribution which describes the relation between the spanwise distributed angle of attack $\alpha(y)$ and the circulation distribution $\gamma(y)$. This relation is only valid for small curved profiles and is based on the assumption that the local circulation is linear dependent on the local angle of attack.

The circulation distribution in wing chord direction is modeled according to BIRNBAUM's first and second distribution functions. Therefore the kinematic flow condition has to be satisfied at two points along the profile. TRUCKENBRODT choses the quarter chord line and the wing trailing edge.

If the wing is replaced by a discrete number of elementary wings M each having a constant circulation in the spanwise direction we get a set of 2M integral equations which describe the relationship between the angle of attack α_v at 2M reference locations of the wing and the the local circulation γ_v as well as the local pitching moment coefficient μ_v at M profiles along the wing span. If local circulation and local pitching moment are approximated by FOURIER polynoms we get the following equations:

for the quarter chord line (index **):

$$\begin{aligned}\alpha_v^{**} = \; & b_{vv} i_{vv}^{**} \gamma_v - \sum_{n=1}^{M}{}' b_{vn} i_{vn}^{**} \gamma_n \\ & + b_{vv} j_{vv}^{**} \mu_v - \sum_{n=1}^{M}{}' b_{vn} j_{vn}^{**} \mu_n\end{aligned} \tag{3.4a}$$

for the trailing edge (index *):

$$\begin{aligned}\alpha_v^{*} = \; & b_{vv} i_{vv}^{*} \gamma_v - \sum_{n=1}^{M}{}' b_{vn} i_{vn}^{*} \gamma_n \\ & + b_{vv} j_{vv}^{*} \mu_v - \sum_{n=1}^{M}{}' b_{vn} j_{vn}^{*} \mu_n\end{aligned} \tag{3.4b}$$

The index "n" indicates the inducing wing element and the index "v" indicates the point where the induction of all wing elements is calculated. The " ' " means that in the

summation $\nu = n$ is not considered.

Adaption to Real-Time Requirements

The coefficients $b_{\upsilon n}$ are only dependent on the value of M and can be calculated according to MULTHOPP. The coefficients $i_{\upsilon n}$ and $j_{\upsilon n}$ are dependent on the geometry of the wing. These 2M equations can be written in a matrix form:

$$\begin{bmatrix} \alpha_1^{**} \\ \vdots \\ \alpha_M^{**} \\ \alpha_1^{*} \\ \vdots \\ \alpha_M^{*} \end{bmatrix} = \begin{bmatrix} K_{1,1} & \cdots & K_{1,M} & K_{1,M+1} & \cdots & K_{1,2M} \\ \vdots & \ddots & \vdots & \vdots & \ddots & \vdots \\ K_{M,1} & \cdots & K_{M,M} & K_{M,M+1} & \cdots & K_{M,2M} \\ K_{M+1,1} & \cdots & K_{M+1,M} & K_{M+1,M+1} & \cdots & K_{M+1,2M} \\ \vdots & \ddots & \vdots & \vdots & \ddots & \vdots \\ K_{2M,1} & \cdots & K_{2M,M} & K_{2M,M+1} & \cdots & K_{2M,2M} \end{bmatrix} \cdot \begin{bmatrix} \gamma_1 \\ \vdots \\ \gamma_M \\ \mu_1 \\ \vdots \\ \mu_M \end{bmatrix} \quad (3.5a)$$

respectively

$$\underline{\alpha} = \underline{\underline{K}} \cdot \underline{\gamma} \quad (3.5b)$$

where $\underline{\alpha}$ is the given angle of attack vector with 2M elements, $\underline{\underline{K}}$ is a 2M x 2M matrix and $\underline{\gamma}$ is an unknown vector with 2M elements, where the first M elements are the local circulation coefficients γ_ν and the second M elements are the local pitching moment coefficients μ_ν. The elements of the matrix $\underline{\underline{K}}$ only depend on the number of reference profiles M and the geometry of the wing. Therefore $\underline{\underline{K}}$ is constant and can be pre-computed for a given aircraft.

The relation between the index of the profile ν and the spanwise coordinate y is given by

$$y_\nu = \frac{b}{2}\cos\vartheta_\nu \qquad \upsilon = 1...M \quad (3.6)$$
$$\vartheta_\nu = \frac{\nu\pi}{M+1}$$

where b is the wing span. Eq. (3.5) has to be solved during each simulation time step by using an equation solving algorithm. For real-time simulation this is not suitable. A faster way of solving eq. (3.5) is given by using the inverse $\underline{\underline{K}}^{-1}$:

$$\underline{\gamma} = \underline{\underline{K}}^{-1} \cdot \underline{\alpha} \quad (3.7)$$

In this case the calculation of the unknown local circulation respectively pitching moment distribution is given by a simple matrix operation, while the inverse of $\underline{\underline{K}}$ can also be pre-computed once in an initialisation procedure.

Combination with real Aircraft Data

The lifting surface theory has two main disadvantages:

- it is linear in the dependance of the angle of attack
- it gives only information about the wing and tail aerodynamics

Therefore this model can only be considered as an approximation of the aerodynamic behaviour of a determined real aircraft. To improve this the lifting surface model is combined with the above described one-point-model which includes very precisely the nonlinear aerodynamic behaviour of the whole aircraft including the influence of control surfaces like rudder, elevator, aileron, flaps etc.. The advantages of both models are combined by using the one-point model for the calculation of the influence of the mean wind and the lifting surface model for the influence of the local deviations from the mean wind. Therefore the influence of local deviations in the angle of attack is calculated by

$$\Delta\underline{\gamma} = \underline{\underline{K}}^{-1} \cdot \Delta\underline{\alpha} \quad (3.8)$$

The deviations of the local coefficients for lift and pitching moment (with reference to the local quarter chord line) at the location ν can be calculated from[14]

$$\Delta c_{L,\nu} = \frac{2b}{\ell_\nu}\Delta\gamma_\nu \quad (3.9)$$

$$\Delta c_{m,\nu} = \frac{2b}{\ell_\nu}\Delta\mu_\nu \quad (3.10)$$

where l_ν is the local aerodynamic chord. The changes in the local coefficient for induced drag Δc_{Di} cannot be calculated in this way because they are nonlinear dependent on α_υ. Therefore the local deviations of the induced drag coefficient must be calculated

$$\Delta c_{Di,\nu} = c_{Di,\nu} - c_{Di,\nu,mean} \quad (3.11)$$

where $c_{Di,\nu,mean}$ is the local drag coefficient calculated for the mean angle of attack $\alpha_{\nu,mean}$ while $c_{Di,\nu}$ is calculated for the local angle of attack

$$\alpha_\nu = \alpha_{mean} + \Delta\alpha_\nu \quad (3.12)$$

The induced total local drag coefficient can be calculated from the pressure distribution along the profile[13]

$$c_{Di,\nu} = \int_0^1 \Delta c_{p,\nu}(\xi)\,\alpha_{i,\nu,total}(\xi)\,d\xi \quad (3.13)$$

with the dimensionless coordinate in wing chord direction

$$\xi = \frac{x - x_{nose,\nu}}{\ell_\nu} \quad (3.14)$$

The total induced angle of attack $\alpha_{i,\nu,total}$ consists of the influence of the circulation distribution along the wing span (self induced) and the influence of wind disturbances (wind induced)

$$\alpha_{i,\nu,total}(\xi) = \alpha_{i,\nu} + \alpha_{W,\nu}(\xi) \quad (3.15)$$

The distribution of the wind angle of attack in wing chord direction can be approximated by a linear function in ξ:

$$\alpha_{W,\nu}(\xi) = a_{0,\nu} + a_{1,\nu}\cdot\xi \quad (3.16)$$

Therefore the local drag coefficient can be calculated according to BEUKENBERG[2]

$$c_{Di,\nu} = \frac{2b}{\ell_\nu}\gamma_\nu \alpha_{i,\nu} + \frac{2b}{\ell_\nu}\left[\gamma_\nu\left[a_{0,\nu}+\frac{1}{4}a_{1,\nu}\right]-a_{1,\nu}\mu_\nu\right] \quad (3.17)$$

where the first expression gives the influence of the self induced drag and the second gives the influence of atmospheric wind disturbances. The coefficients a_0 and a_1 for each location ν are given by the wind angle of attack at the quarter chord line α_W^{**} and at the trailing edge α_W^{*}:

$$a_{0,\nu} = \frac{1}{3}\left[4\alpha_{W,\nu}^{**} - \alpha_{W,\nu}^{*}\right] \quad (3.18a)$$

$$a_{1,\nu} = \frac{4}{3}\left[\alpha_{W,\nu}^{*} - \alpha_{W,\nu}^{**}\right] \quad (3.18b)$$

The wind angle of attack is given by SCHÄNZER[12]

$$\alpha_{W,\nu}(\xi) = -\frac{u_{Wg,\nu}(\xi)}{V}\sin\gamma - \frac{w_{Wg,\nu}(\xi)}{V}\cos\gamma \quad (3.19)$$

where u_{Wg} and w_{Wg} are the horizontal and vertical components of the wind vector given in geodetic coordinates and γ is the flight path angle. The last unkown expression in eq. (3.17) is the self induced angle of attack at each location ν, which can be calculated from[14]

$$\alpha_{i,\nu} = b_{\nu\nu}\gamma_\nu - \sum_{n=1}^{M}{}' b_{\nu n}\gamma_n \quad (3.20)$$

By this eq. (3.17) becomes

$$c_{Di,\nu} = \frac{2b}{\ell_\nu}\gamma_\nu \alpha_{i,\nu} + \frac{2b}{\ell_\nu}\left[\gamma_\nu\alpha_{W,\nu}^{**} - \frac{4}{3}\left(\alpha_{W,\nu}^{*} - \alpha_{W,\nu}^{**}\right)\mu_\nu\right] \quad (3.21)$$

To get the distribution of the local deviations of the drag coefficient from eq. (3.11) this procedure has to be done for total angle of attack as well as for the mean angle of attack.

According to HUMMEL[6] the lift coefficient for the whole wing is given by

$$C_L = \frac{\pi\Lambda}{M+1}\sum_{\nu=1}^{M}\gamma_\nu \sin\vartheta_\nu \quad (3.22)$$

With eq. (3.9) we get for the deviation

$$\Delta C_L = \frac{\pi\Lambda}{M+1}\sum_{\nu=1}^{M}\frac{\ell_\nu}{2b}\Delta c_{L,\nu}\sin\vartheta_\nu \quad (3.23)$$

The coefficient for induced drag for the whole wing can be calculated in a similar way:

$$\Delta C_{Di} = \frac{\pi\Lambda}{M+1}\sum_{\nu=1}^{M}\frac{\ell_\nu}{2b}\Delta c_{Di,\nu}\sin\vartheta_\nu \quad (3.24)$$

The coefficient for the pitching moment with respect to a chosen reference axis can be calculated from

$$\Delta C_{m,nose} = \frac{\pi\Lambda}{M+1}\sum_{\nu=1}^{M}\left[\frac{\ell_\nu}{2b}\left(\Delta c_{m,\nu}\frac{\ell_\nu}{\ell_\mu} - \Delta c_{L,\nu}\frac{x_{25}}{\ell_\mu}\right)\sin\vartheta_\nu\right] \quad (3.25)$$

where x_{25} is the local distance of the quarter chord line from the reference axis, Λ is the wing aspect ratio and l_μ is the mean aerodynamic chord:

$$\Lambda = \frac{b^2}{A} \quad (3.26)$$

$$\ell_\mu = \frac{1}{A}\int_{-s}^{s}\ell^2(y)\,dy \quad (3.27)$$

The coefficients for rolling and yawing moments can be calculated from

$$\Delta C_\ell = -\frac{\pi\Lambda}{M+1}\sum_{\nu=1}^{M}\frac{\ell_\nu}{2b}\Delta c_{L,\nu}\,\eta_\nu \sin\vartheta_\nu \quad (3.28)$$

$$\Delta C_n = \frac{\pi\Lambda}{M+1}\sum_{\nu=1}^{M}\frac{\ell_\nu}{2b}\Delta c_{Di,\nu}\,\eta_\nu \sin\vartheta_\nu \quad (3.29)$$

This procedure has to be done for the wing and the horizontal tail. To underline the precision of the lifting surface model the resulting values of the local circulation are compared with references given by literature[6]. The results given in tab. 3.1 demonstrate a good accordance.

Tab. 3.1 Local circulation and pitching moment

$\Lambda = 5$, $\ell(y)$ = constant, $\varphi = 45°$, $\alpha = 1$

	reference	lifting surface model	error [%]
$\gamma_{1,7}$	0,238	0,2371	-0,4
$\gamma_{2,6}$	0,371	0,3700	-0,3
$\gamma_{3,5}$	0,380	0,3791	-0,2
γ_4	0,321	0,3198	-0,4
$\mu_{1,7}$	0,0311	0,0314	1,0
$\mu_{2,6}$	0,0097	0,0098	1,0
$\mu_{3,5}$	-0,0002	-0,0002	0,0
μ_4	-0,0071	-0,0071	0,0

Fig. 3.3 shows the circulation distribution as well as the angle of attack distribution for a wing right in the center of a wake vortex flow for M = 31[8].

The accuracy of the lifting surface model depends on the number of reference points along wing and tail in relation to the ratio of the wave length of the wind disturbance λ to the semi wing span s. For an error analysis the total rolling moment was calculated for a sine shaped wind distribution

with a wave length equal to the wing span which gives a ratio $\lambda/s = 2$. The number of reference points is varied between M = 11 and M = 99, see fig. 3.4.

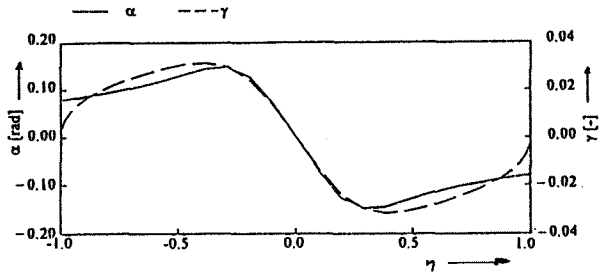

Fig. 3.3 Distribution of circulation and angle of attack for a wing in the center of a vortex flow[8]

As reference for the error calculation the solution for M = 201 was chosen. As expected for low values M the error decreases sharply with an increasing number of reference points. With an error between 17 % for 11 reference profiles and below 1 % for 99 reference profiles the lifting surface shows a good performance. For practical use the number of reference points should be adapted to the shortest wavelength of the wind disturbance. For wake vortex investigations of an encountering aircraft with a wing span of about 15 m the minimum number of reference points should be about 31.

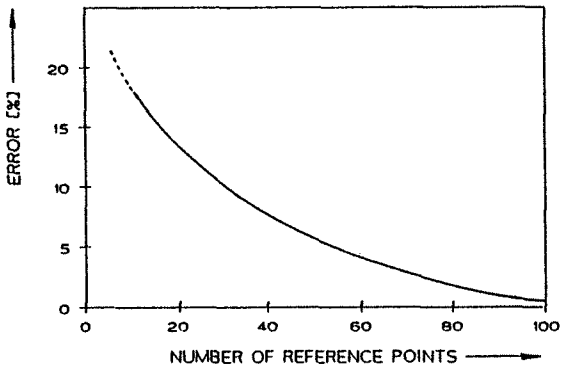

Fig. 3.4 Error of the lifting surface model ($\lambda/s = 2$)[7]

4. Wind Models

4.1 General

Parallel to the development of multi-point aerodynamic models three-dimensional real-time wind and turbulence models have been developed. During the simulation the wind vector has to be calculated at discrete locations of the aircraft, both for the four-point model and for the lifting surface model. For different research tasks different wind models are necessary. The scenario with the strongest requirements concerning the computation performance in a real-time simulation are complex phenomena like microburst or wake vortices.

Fig. 4.1 shows a typical thunderstorm scenario. A well known approach for the calculation of wind vectors for a microburst was presented by ZHU[16]. This model is based on circular shaped vorticity layers which are distributed at different altitudes in the center of the microburst. The problem of wind vector determination using this model is the calculation of induced velocities in real-time, which often cannot be solved within the limited performance of the simulation computer.

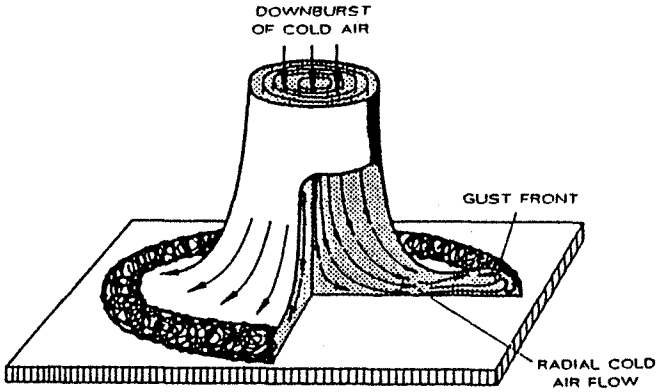

Fig. 4.1 Microburst scenario[10]

A simplified three-dimensional model based on a discrete number of ring-vortices was developed by BAUSCHAT[1]. The parameters of the model can be adapted to different downburst scenarios.The required computation power was matched by a VAX-4000-300 used as simulation computer for a standard downburst scenario. As the complexity of some of the wind models expired the real-time capability of the simulation computer a new development based on pre-computed wind models was initiated, which can be applied under real-time conditions. This new kind of model is named matrix-windmodel.

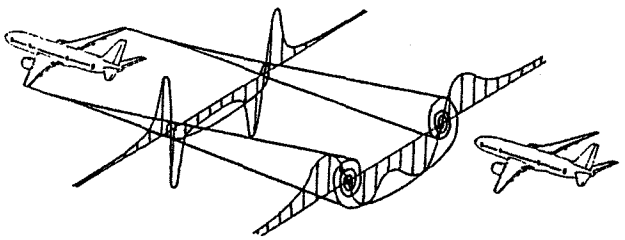

Fig. 4.2 Aircraft encountering wake turbulence

For simulation investigations concerning two landing aircraft on the same glide path a three-dimensional wake vortex model was developed. Fig. 4.2 shows an aircraft encountering wake turbulence. Typical attributes of wake vortices are:

- generated by other aircraft
- induced wind velocities depend on the distance to the vortex generating aircraft (vortex age)
- significant wind changes within small sized ranges
- induced wind velocities depend upon the vortex movement
- short wavelength in the meter range

Because wake vortices are an instationary phenomenon and because the induced wind velocities depend on the distance between the generating and the encountering aircraft this complex wind model cannot be pre-computed and stored as a wind matrix. Therefore a real-time capable mathematical algorithm has been developed, which describes the velocity distribution of the vortex flow field by an analytical approximation.

4.2 Matrix-Wind Model

The idea of the matrix-wind model developed by KNÜPPEL[9] is to execute the whole wind model computation offline and to store the computed wind field in a matrix. For the simulation of a typical landing approach with an initial fixed position in 10 km distance to the threshold and a resolution of the stored wind vectors of 10 m in the pre-computed wind matrix, the amount of storage is more than 50 Mbyte. Fig. 4.3 shows a typical matrix shape for a take-off and landing area.

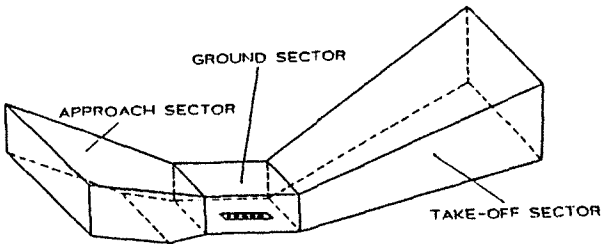

Fig. 4.3 Typical take-off and landing area of the matrix-wind model

Modern computer systems allow the storage of the pre-computed wind matrix in the random access memory (RAM). The calculation of the wind vectors at the determined locations of the aircraft is done by an interpolation algorithm, see fig. 4.4.

If the large amount of RAM is not avaiable on the simulation computer, this capacity problem can be solved by storing the wind matrix on a hard-disk and reading the actual required parts of the wind matrix (called wind-boxes) when they are needed. A special management program using a forecast algorithm is responsible for the replacement of actual required wind-boxes in the RAM.

The advantages of this matrix-windmodel are the following:

- real-time simulation of pre-computed, complex spatial wind, gust and turbulence scenarios
- complexity of the model not limited by the real-time computation performance
- multi-point models can be calculated in real-time with only few additional computations
- inclusion of measured flight test data is possible
- superposition of different models is possible, e.g. the simulation of several different microbursts in the same approach area

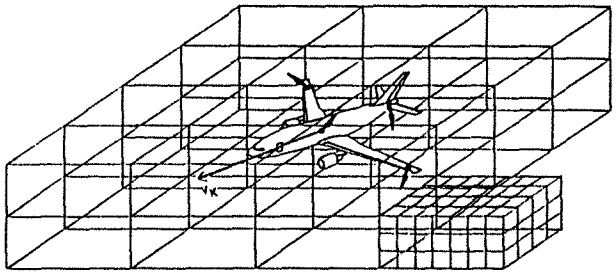

Fig. 4.4 Aircraft in the wind-boxes of the matrix-wind-model

4.3 Microburst Model

A typical application of the matrix-wind model is the microburst scenario. These extreme wind conditions have caused several severe aircraft accidents during take-off and landing approach[11]. Therefore airlines involved simplified microburst models in their simulator training. These models are used to familiarize the flight crews to the special situation of encountering and recognizing microburst situations. However, these models often are only simple reconstructions of the real situation.

Fig. 4.5 shows a typical accident situation during a landing approach at the Kennedy Airport in New York, 1975. Two different microbursts influenced the landing approach of a Boeing 727. The aircraft failed with the attempt of a go-around procedure and crashed before the threshold.

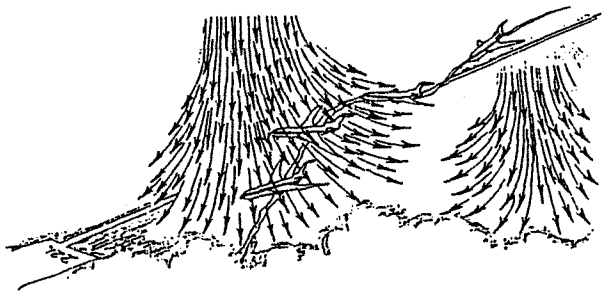

Fig. 4.5 Kennedy airport accident scenario[11]

The above mentioned three-dimensional ring-vortex microburst from BAUSCHAT[1] can be used to describe this microburst situation. Fig. 4.6 shows the arrangement of

ring vortices for a single microburst. The wind vectors in the vertical plane along a landing approach flight path show the typical change from head- to tailwind and from up- to downwind along the flight path. Only with a spatial model this cross-wind effects can be simulated realistically, which is most important for realistic pilot's workload during landing approach under these conditions.

The ring-vortex approach allows the calculation of a complete spatial model, e.g. based on accident data measured along the flight path of an aircraft. A special optimization algorithm is used to adapt the model parameters to the measured data. The combination of matrix-wind model and ring-vortex microburst model enables the simulation of very sophisticated spatial microburst scenarios with a sample step width in the meter range.

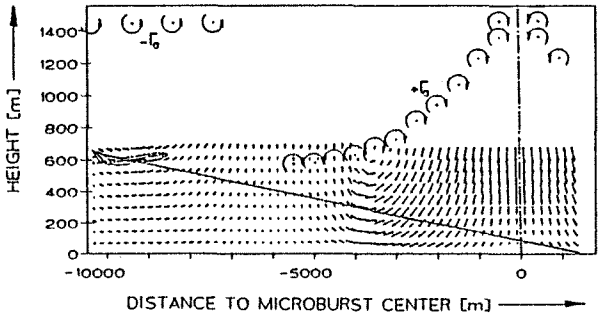

Fig. 4.6 Ring-vortex model for microburst[1]

4.4 Wake Vortex Model

To avoid dangerous wake vortex encounter in the landing segment, a separation rule has been introduced called Wake Turbulence Classification which defines minimum separation distances of two landing aircraft from 3 to 6 nm, depending on the weight of the vortex generating and the following aircraft.

As a result of the intensive growth of the international airtraffic this classification has become more and more a limiting factor for the economical operation of international airports. To improve this situation, a decrease of the separation minima is desirable without a loss of flight safety. For a solution detailed knowledge of the aircraft behaviour in a wake vortex flow is required.

For these investigations the pilot's reaction is important. Therefore flight simulation studies with the pilot in the loop are necessary so that the wake vortex model has to be real-time capable.

Fig. 4.7[2] shows the life cycles of a wake vortex, which can be simplified by three stages:

1. roll up stage, which takes only few time,
2. transition stage, where the influence of friction causes a decrease of the maximum velocity and a growth of the vortex core,
3. decay stage, where the whole kinetic energy is consumed by friction and the vortex dissipates into random turbulence.

After their generation at the wing trailing edge, the vortices sink due to their mutual induced velocity. The vortex cores, which are positioned at the wing tips at the first moment, move in the lateral direction, see fig. 4.8. In proximity to the ground, the vertical movement converts into a horizontal movement and the vortices drift apart. The lateral vortex velocity is superposed by crosswind, so that the vortices may move from one runway to a nearby parallel runway or stay on the runway.

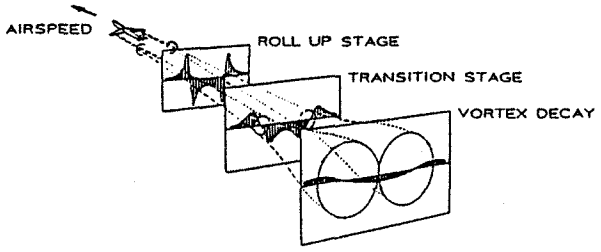

Fig. 4.7 The three vortex stages[2]

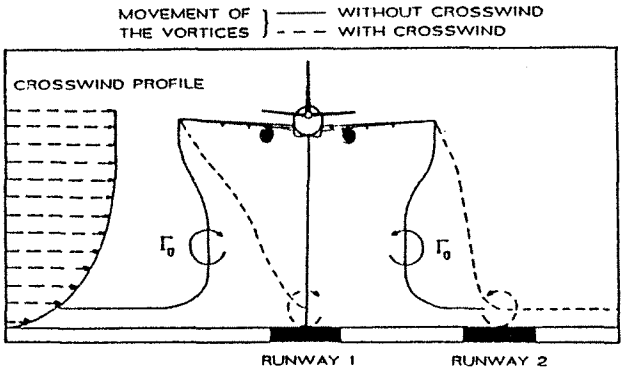

Fig. 4.8 Vortex movement behind the aircraft[5]

For realistic simulator investigations a precise vortex model is necessary. Investigations of the velocity distribution in the vortex flow have led to several approximations, which mostly however do not describe the vortex aging process exactly. According to the progress in the development of fast digital computers, the description of the vortex flow field by numerical simulation has become more and more interesting. Therefore a new spatial wake vortex model has been developed by HEINTSCH[5] which describes the vortex generation and expansion as well as the vortex movement. The main model parameters are the weight and the geometric dimensions of the vortex generating aircraft and the age of the vortex.

Based on KUTTA-JOUKOVSKY the spanwise distribution of local lift can be described by a relevant circulation distribution. According to the HELMHOLTZ's vortex laws each vortex forms a closed ring with constant circulation and consists of a bound vortex on the wing, two counterrotating free vortices and an initial vortex, see fig. 4.9. HELMHOLTZ states, that the decrease of bound circulation in the spanwise direction corresponds to an increase of free circulation in the vortex sheet.

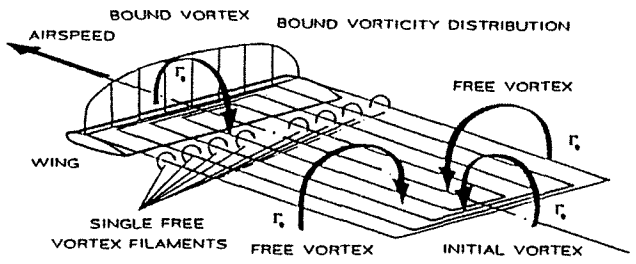

Fig. 4.9 Vortex system behind a wing[5]

The continuously distributed vorticity can be approximated by a discrete vortex system, which results in a set of single bound and free vortices, whose strength is a function of total lift, airspeed, air density and lift distribution. The velocity distribution induced by the whole vortex system can be calculated according to the law of BIOT-SAVART by superposing the influence of every single vortex (single-vortex simulation). The numerical integration of these equations leads to the roll up of the vortex sheet into two counterrotating spirals, see fig. 4.10.

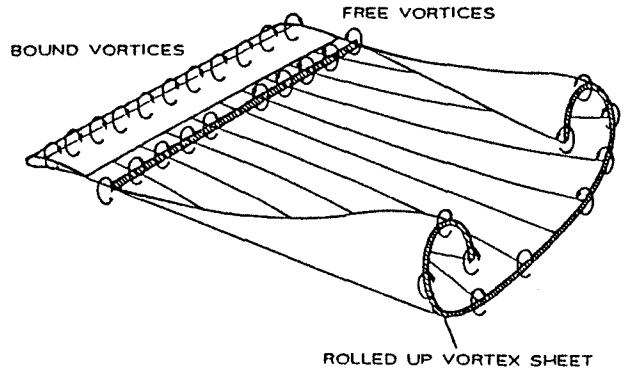

Fig. 4.10 Roll up of the vortex sheet[5]

To describe the roll up process realistically, this model requires an extreme numerical expense. The simulation of one real second requires more than 10 hours of CPU time on a VAX-4000-300 computer. This high amount of computation time makes the single-vortex method insuitable for the use as an engineering model in real-time aircraft flight simulation. However, in comparison to real measurements which have been carried out under the supervision of the FEDERAL AVIATION ADMINISTRATION (FAA) in the United States 1970-1973 this model shows good results in the characteristical parameters maximum velocity and vortex core radius, see tab. 4.1[5].

Tab. 4.1 Measured wake vortex parameters in comparison to the single-vortex simulation[5]

vortex age [s]	maximum tangential velocity [m/s]		vortex core radius [m]	
	measurement	simulation	measurement	simulation
5	45	45	0.35	0.5
17	34	32	0.5	0.7
26	30	28	0.7	0.9

Using the single-vortex simulation as a reference a more simple description of the wake vortex flow has been developed by HEINTSCH[5], which describes the velocity distribution in a plane normal to the vortex axis as an analytical function of the distance to the vortex center and time. The parameters of this model are simple functions of time and have been found by an optimization procedure. Only by this the complex time dependant wind field of a wake vortex flow can by simulated realistically under real-time conditions on standard simulation computer systems.

5. Simulation Results

A typical test procedure for the four-point model is the encounter of a 1-cos shaped vertical upwind gust. The simulation runs were carried out with the research flight simulator at Braunschweig University of Technology. The diameter of the gust was chosen to 500 m which leads to a wave length ratio $\lambda/s = 22$. Fig. 5.1 shows the ground track with the one-point and the four-point model in comparison for fixed controls to avoid overlapping of pilot influences. The differences are evident and were clearly identified by the pilot in simulations with the pilot in the loop as well.

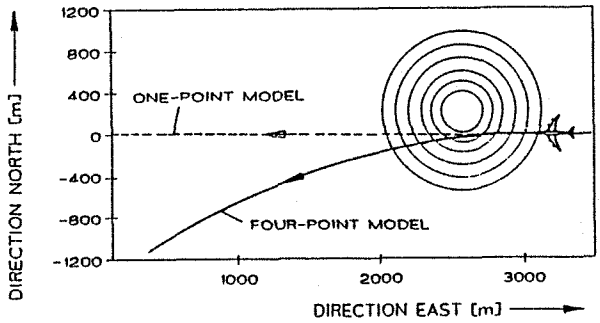

Fig. 5.1 Aircraft encountering 1-cos gust

Fig. 5.2 shows the EULER angles for both models in comparison, which are significantly different, especially in the lateral motion, because here the one-point model has no input signal. Compared to the one-point model the pitch reaction of the four-point model is reduced and shows a

contrary reaction at the first seconds when entering the gust, because at the first moment only the wing is influenced by the wind disturbances.

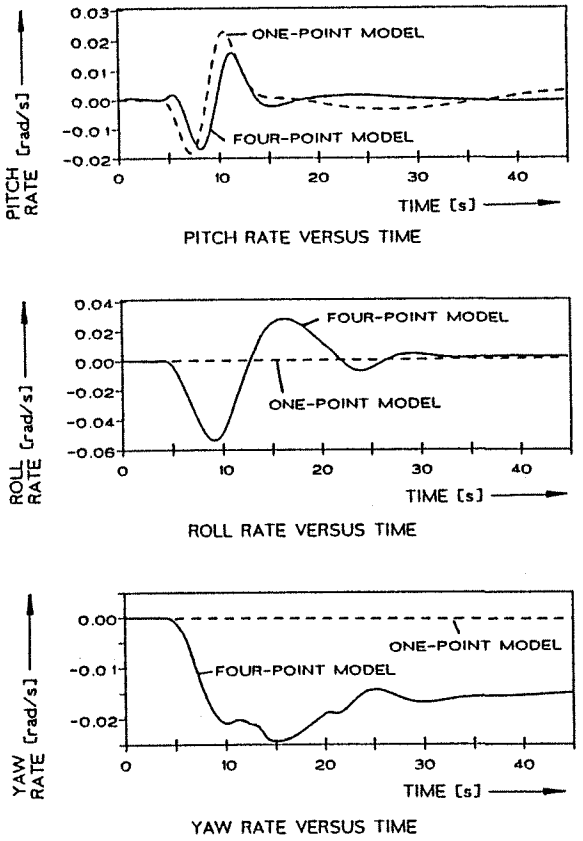

Fig. 5.2 Aircraft response to 1-cos vertical gust

Some other simulation runs were carried out with a typical wake vortex encountering procedure. The vortex generating aircraft was a wide body transport aircraft with a weight of 265 t, approaching the runway at an airspeed of $V = 70\ ms^{-1}$. The encountering aircraft was a commuter aircraft with a weight of 5.5 t and was approaching the same runway at the same speed. It was following in a distance of 11 km, which is accordance with the Wake Turbulence Classification. The simulation was started with the encountering commuter aircraft in landing configuration stabilized on the glide path. The aircraft was piloted by two research pilots which are well trained on this aircraft. The pilot had the order to maintain the glide path as best as possible, his guidance information was given by a cross pointer. The height of the wake vortex core was about 25 m, which is reached when the vortices sink to the ground.

Fig 5.3 shows some results of a simulation when the pilot hit the vortex near his core. The aircraft shows a very strong reaction in the bank angle which reaches up to 20 degree. The pilot had severe problems to control the aircraft. The reason was probably that the vortex induced rolling moment was positive at the first moment but then turned rapidly into negative. The pilot's reaction in the aileron lever deflection was negative at the first moment to compensate the induced rolling moment, but he didn't expect the change in the sign. So in the following he had to command up to 60 degree at the control column, which means that the handling limits were nearly reached. Finally the pilot decided to perform a go-around maneuver.

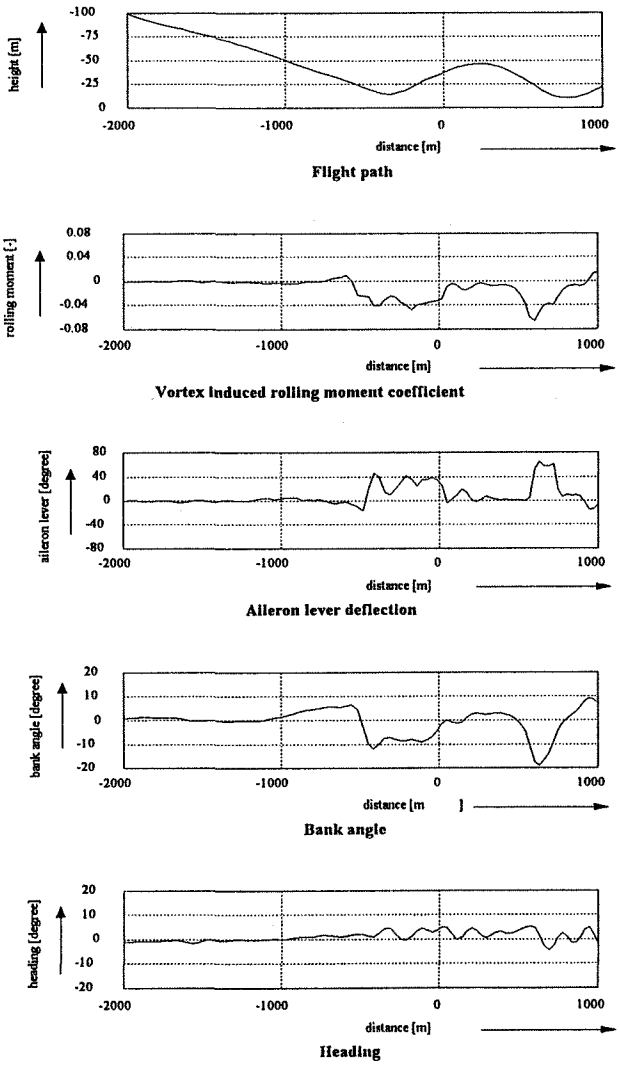

Fig. 5.3 Aircraft encountering wake vortex

6. Conclusions

The influence of atmospheric perturbations on aircraft motion is of great interest since the beginning. The scale of the atmospheric perturbations is an significant parameter concerning the required complexity for the description of the wind-aircraft interaction. In the short scale range of atmospheric perturbations the use of an one-point model is not suitable. To get realistic results, the wind influence along the whole surface of the aircraft has to be considered. For real-time simulation practise an approximation which just considers the wind influence at several characteristical points of the aircraft should be adopted. The aircraft

aerodynamic four-point model and the matrix-windmodel together with pre-computable three-dimensional wind models like complex microburst scenarios have provided a sophisticated solution which is real-time capable. The validity of the four-point model is restricted to wave lengths not shorter than the sixfold size of the aircraft wing span.

Based on the linear lifting surface theory an aerodynamic model was developed, which takes into account the spatial distribution of wind vectors along the wing and the tail plane span. This model considers only the local deviations from the mean wind. The influence of the mean wind on the aircraft aerodynamic is calculated by the one-point model, using real test data stored in look-up tables. Therefore the individual aircraft characteristics combined with accurate consideration of a spatial wind field give a precise description of the wind-aircraft interaction.

For the simulation of aircraft encountering a wake vortex the wind model cannot be precomputed because of the vortex aging process. Based on a complex vortex simulation as a reference an analytical function was developed which realistically describes the vortex flow field and the vortex aging process very precisely. As the vortex core radius is in the meter range, the four-point model is not precise enough to calculate the forces and moments induced by the vortex flow field.

All models have been applied on the research simulator of the Technical University of Braunschweig. Some results have been presented and the advantages of the developed models were demonstrated. Future tasks will show the benefit of this work for the simulation quality, which is important not only for research tasks but also for training and development applications. In the near future the lifting surface aerodynamic model will be implemented on the Airbus A340 Full-Flight-Simulator at Berlin University of Technology.

Acknowledgements

The content of this paper is a result of the research work of the authors and their colleagues at the Institute of Flight Guidance and Control of Braunschweig University of Technology within the "Sonderforschungsbereich 212 Sicherheit im Luftverkehr" sponsored by the German Research Community DFG.

References

(1) BAUSCHAT, M. Entwicklung eines dreidimensionalen mathematischen Gewittermodells zur Untersuchung des Flugverhaltens in Gewitterstürmen, master thesis at the Institute of Flight Guidance and Control, Technical University of Braunschweig, 1988

(2) BEUKENBERG, M. Beiträge zu Aerodynamik und Flugmechanik des Formationsfluges, doctor thesis at the Faculty for Mechanical Engineering and Electronics, Technical University of Braunschweig, 1983

(3) BROCKHAUS, R. A Mathematical Multi-Point Model for Aircraft Motion in Moving Air, Zeitschrift für Flugwissenschaften und Weltraumforschung, No. 3, 1987

(4) FEGEL, E. Integration eines Mehrpunktsimulationsmodells in das 6-Freiheitsgrad Simulationsprogramm des Instituts für Flugführung, master thesis at the Institute of Flight Guidance and Control, Technical University of Braunschweig, 1989

(5) HEINTSCH, T. Beiträge zur Modellierung von Wirbelschleppen zur Untersuchung des Flugzeugverhaltens beim Landeanflug, doctor thesis at the Faculty for Mechanical Engineering and Electronics, Technical University of Braunschweig, 1994

(6) HUMMEL, D. Aerodynamik II, lecture notes, Institute of Aerodynamics, Technical University of Braunschweig, 1979

(7) KINDEL, W. & HEINTSCH, T. Three-Dimensional Real-Time Models for the Interaction between Wind and Aircraft, International Conference "Flight Simulation", Moscow, 1992

(8) KINDEL, W. & HEINTSCH, T. Influence of Wake Vortices on a Landing Aircraft - A Task for Real-Time-Flightsimulation, International Conference "Aircraft Flight Safety", Moscow, 1993

(9) KNÜPPEL, A. Untersuchungen zum Einsatz von Matrix-Windmodellen in der Echtzeitsimulation, master thesis at the Institute of Flight Guidance & Control, Technical University of Braunschweig, 1988

(10) KRAUSPE, P. Beiträge zur Längsbewegung von Flugzeugen in Windscherungen, doctor thesis at the Faculty for Mechanical Engineering and Electronics, Technical University of Braunschweig, 1983

(11) NATIONAL TRANSPORTATION SAFETY BOARD Aircraft Accident Report NTSB-AAR-76-8, Washington D.C., New York, June 24, 1975

(12) SCHÄNZER, G. Einführung in die Flugphysik, lecture notes, Institute of Flight Guidance & Control, Technical University of Braunschweig, 1991

(13) SCHLICHTING, H. & TRUCKENBRODT, E. Aerodynamik des Flugzeuges, Band II, Springer-Verlag, Berlin Heidelberg New York, 1969

(14) TRUCKENBRODT, E. Tragflächentheorie bei inkompressibler Strömung, WGL Jahrbuch, 1953

(15) ZHU, S. & ETKIN, B. Fluid-Dynamic Model of a Downburst, UTIAS-Report Nr. 271, April 1983